Appendix 3 - Corrosion and Corrosion Fatigue of Vitreloy Glasses Containing Low Fractions of Late Transition Metals

The text and figures of this appendix draw heavily on a paper submitted and under review in Scripta Materialia entitled "Corrosion and Corrosion Fatigue of Vitreloy Glasses Containing Low Fractions of Late Transition Metals." The authors are A. Wiest, G.Y. Wang, L.Huang, S. Roberts, M.D. Demetriou, P.K. Liaw, and W.L. Johnson.

Corrosion resistance and fatigue performance of Vitreloy glasses with low fractions of late transition metals (LTM) in 0.6M NaCl are investigated and compared to a traditional Vitreloy glass and other crystalline alloys. Low LTM Vitreloy glasses exhibit 1/10 the corrosion rates of the other alloys. Corrosion fatigue performance of present alloys is found to be <10% of their yield strength at 10^7 cycles. The poor corrosion fatigue performance of the present alloys is likely due to low fracture toughness of the passive layer.

Owing to the lack of long range order in their atomic structure and the absence of microscopic defects such as vacancies, dislocation, or grain boundaries that typically arise in crystalline microstructures, bulk metallic glasses (BMG) demonstrate a unique combination of mechanical properties, such as high strength, high hardness, and a high elastic strain limit [1-4]. The lack of electrochemically active sites, provided by the absence of microstructural defects, has long been thought to give rise to exceptional resistance to corrosion and chemical attack. Some BMG alloys based on noble metals indeed demonstrate superb corrosion resistance [5], however, the resistance to corrosion is not universally high for all BMG alloys. Zr based BMG of the Vitreloy alloy family

were found to exhibit corrosion resistance in saline solutions higher than most crystalline engineering metals, however on par with the most advanced corrosion resistant metals. For example, the corrosion resistance of ZrTiNiCuAl glass (Vitreloy 105) in phosphate buffered saline (PBS) was found to be on par or slightly lower than widely used metallic biomaterials such as stainless steels, Ti-6Al-4V, and CoCrMo [6]. Despite the generally good corrosion behavior of Vitreloy type BMG, their behavior in stress corrosion environments, specifically cyclic stress (fatigue) corrosion environments, is rather poor. The stresses at which Vitreloy type BMG endure 10^7 cycles in saline solutions was found to be just 10 - 20% of their corresponding values in air [7,8]. We investigate the corrosion and corrosion fatigue behavior of certain Vitreloy alloy variants in a 0.6M saline environment (simulated sea water) and contrast it to traditional Vitreloy alloys and other metals used in marine applications. We demonstrate that small variations in the Vitreloy alloy composition can lead to dramatic improvements in corrosion resistance. The improvement in corrosion resistance, however, is not accompanied by an analogous improvement in corrosion fatigue endurance, thereby revealing that the two processes are controlled by different physical mechanisms.

A series of Vitreloy type BMG compositions with low atomic fractions of LTM have recently been reported [9]. Many of these alloys were found to exhibit a combination of exceptionally large supercooled liquid region (SCLR) and good glass forming ability. Notable examples include the ternary $Zr_{35}Ti_{30}Be_{35}$ and quaternary $Zr_{35}Ti_{30}Be_{29}Co_6$, with SCLR of 120 °C and 150 °C and critical casting thicknesses of 6mm and 15mm, respectively. Owing to the low LTM atomic fractions, these compositions were thought to also exhibit good corrosion characteristics. The corrosion and corrosion fatigue

behavior of $Zr_{35}Ti_{30}Be_{35}$ and $Zr_{35}Ti_{30}Be_{29}Co_6$ is investigated here, and is contrasted to $Zr_{52.5}Cu_{17.9}Ni_{14.6}Al_{10}Ti_5$, a traditional Vitreloy alloy (Vit105) with a much higher LTM atomic fraction. The measured values are also contrasted to three traditional metallic alloys used in sea water environments: 18/8 stainless steel, Monel (Cu-Ni-based), and Alclad (Al-based) [10].

Alloys $Zr_{35}Ti_{30}Be_{35}$ and $Zr_{35}Ti_{30}Be_{29}Co_6$ were prepared by arc melting elements of >99.9% purity on a water cooled Cu plate in Ti-gettered argon atmosphere. 3mm diameter amorphous rods of $Zr_{35}Ti_{30}Be_{29}Co_6$ and 2mm diameter amorphous rods of $Zr_{35}Ti_{30}Be_{35}$ were cast using an Edmund Buhler mini arc melter suction casting setup. The amorphous nature of the rods was verified using X-ray diffraction and differential scanning calorimetry (DSC).

Cyclic anodic polarization experiments were conducted on unloaded samples of $Zr_{35}Ti_{30}Be_{35}$ and $Zr_{35}Ti_{30}Be_{29}Co_6$ in 0.6M NaCl solution at a scan rate of 0.167 mV/s. Data for Vit 105 was gathered from the study of Morrison et al. [7]. E_{pit}, the pitting potential, and E_{corr}, the steady state corrosion potential, were measured multiple times for each sample. In between measurements, samples were polished with 1200 grit sandpaper in order to remove the reaction layer. Corrosion rates were calculated from corrosion current density measurements. A more detailed description of the experimental method can be found in [6-7]. The averaged cyclic anodic polarization curves for the three alloys are presented in Figure A3.1. Average E_{pit} and E_{corr} values for each alloy along with corrosion rates are tabulated in Table A3.1.

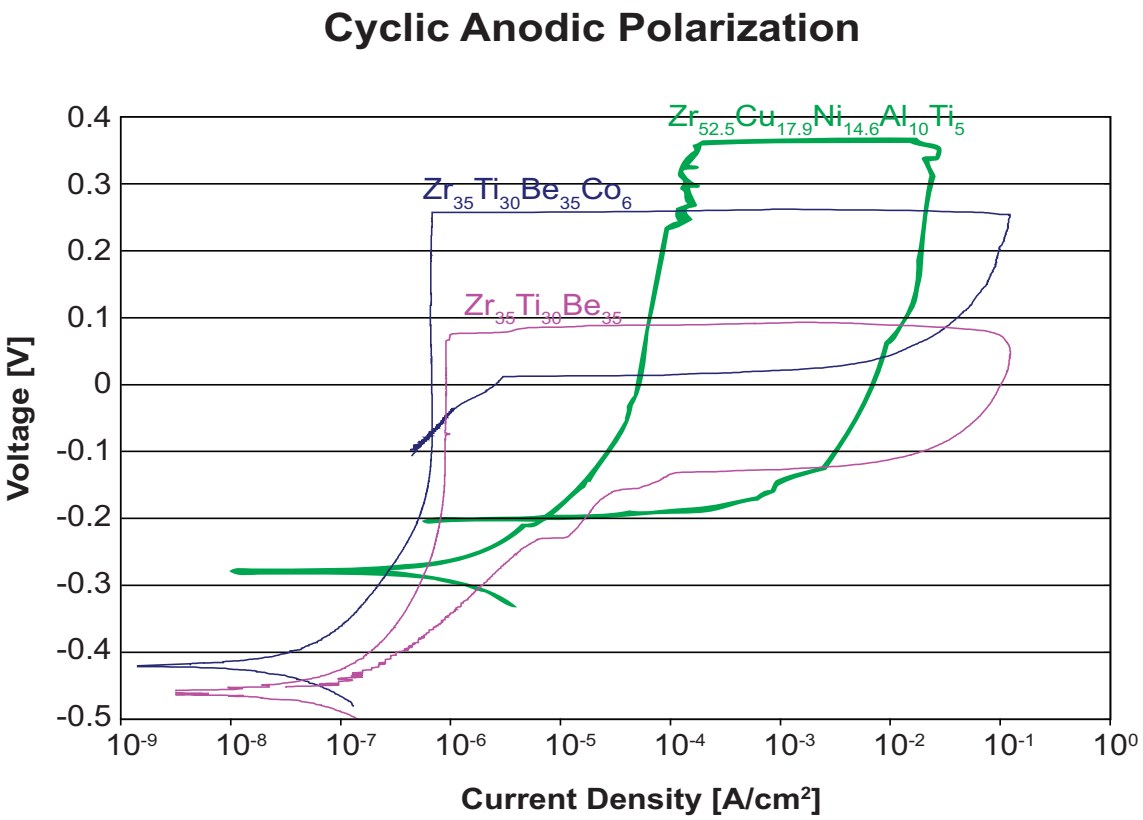

Figure A3.1: Cyclic anodic polarization curves of $Zr_{52.5}Cu_{17.9}Ni_{14.6}Al_{10}Ti_5$, $Zr_{35}Ti_{30}Be_{29}Co_6$, and $Zr_{35}Ti_{30}Be_{35}$ in 0.6M NaCl solution at a scan rate of 0.167 mV/s.

Table A3.1: Data for corrosion and corrosion fatigue in 0.6M NaCl. Fatigue values are the stress amplitudes at which the samples endured 10^7 loading cycles normalized by the material yield strength. The yield strengths of $Zr_{35}Ti_{30}Be_{35}$, $Zr_{35}Ti_{30}Be_{29}Co_6$, and $Zr_{52.5}Cu_{17.9}Ni_{14.6}Al_{10}Ti_5$ are 1850 MPa [22], 1800 MPa [22], and 1700 MPa [7], respectively. Corrosion data for 18/8 Stainless Steel, annealed Monel, and Alclad 24S-T are taken from [10], while data for fatigue in air and 0.6M NaCl are taken from [11-15].

	E_{corr} [mV]	E_{pit} [mV]	corrosion rate [μm per year]	Fatigue (Air) [% strength]	Fatigue (0.6M NaCl) [%strength]
$Zr_{35}Ti_{30}Be_{35}$	-445±42	84.5±23.5	0.871 ±.266	27%	8%
$Zr_{35}Ti_{30}Be_{29}Co_6$	-424±8	257±64	0.544 ±.215	28%	6%
$Zr_{52.5}Cu_{17.9}Ni_{14.6}Al_{10}Ti_5$	-264	324	29±6	25%	6%
18/8 Stainless Steel			13	25%	15%
Monel - Annealed			15.2	40%	35%
Alclad 24S-T			11.2	20%	10%

Fatigue and corrosion fatigue measurements were conducted on 3mm diameter x 6mm tall rods of $Zr_{35}Ti_{30}Be_{29}Co_6$ and 2mm diameter x 4mm tall rods of $Zr_{35}Ti_{30}Be_{35}$ in a compression-compression loading geometry at 10 Hz using a stress ratio

$R = \sigma_{min}/\sigma_{max} = 0.1$. For Vit 105, four-point bending fatigue and corrosion fatigue data from the study of Morrison et al. [7] were utilized. Even though compression-compression and four-point bending fatigue experiments often result in somewhat different endurance limits, the relative drop in the endurance limits between air and saline environments, which is of interest here, is not expected to be dramatically different in the two tests. The S/N curves for the three alloys in air and saline environments are presented in figure A3.2. The ratio of fatigue limit to yield stress in air and in saline solution for the three BMG are listed in Table A3.1. Data for 18/8 stainless steel, Alclad 24S-T and Monel taken from Atlas of Fatigue Curves and other sources [11-15] are also displayed in Table A3.1.

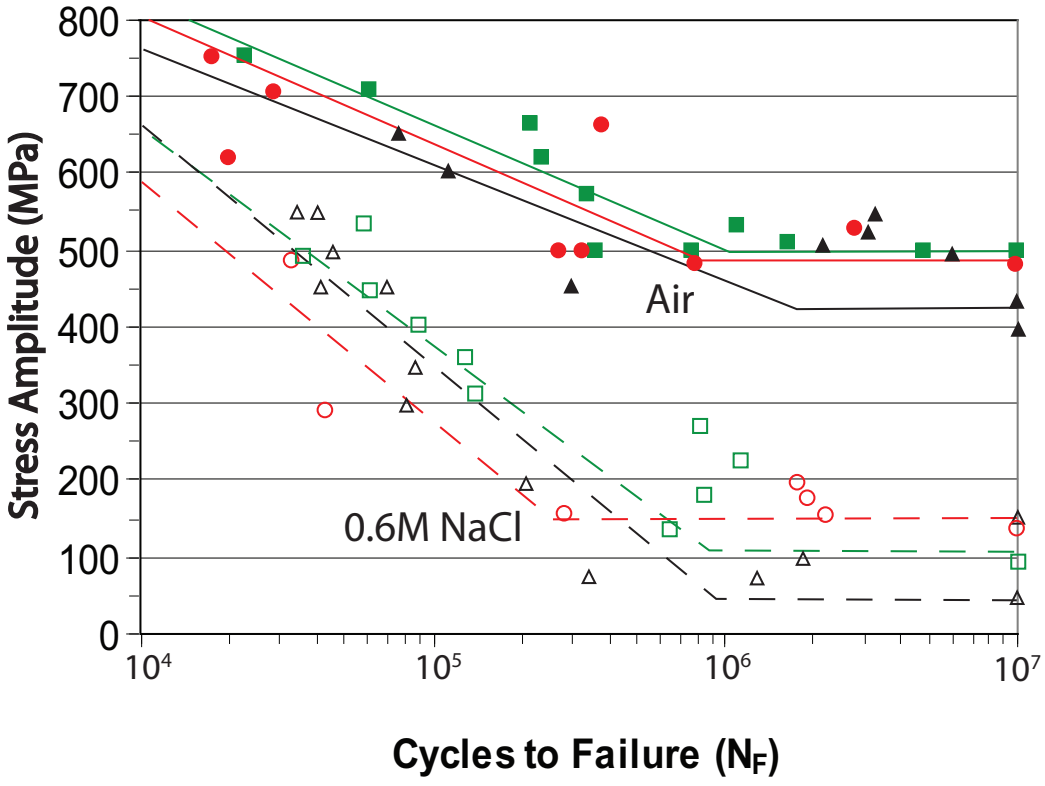

Figure A3.2: Fatigue performance in air (▲ $Zr_{52.5}Cu_{17.9}Ni_{14.6}Al_{10}Ti_5$, ■ $Zr_{35}Ti_{30}Be_{29}Co_6$, and ● $Zr_{35}Ti_{30}Be_{35}$) and in 0.6M NaCl (Δ $Zr_{52.5}Cu_{17.9}Ni_{14.6}Al_{10}Ti_5$, □ $Zr_{35}Ti_{30}Be_{29}Co_6$, and ○ $Zr_{35}Ti_{30}Be_{35}$) at a frequency of 10 Hz and R = 0.1. $Zr_{52.5}Cu_{17.9}Ni_{14.6}Al_{10}Ti_5$ is tested in four-point bending geometry (data taken from [9]). $Zr_{35}Ti_{30}Be_{29}Co_6$ and $Zr_{35}Ti_{30}Be_{35}$ are tested in compression-compression geometry (present study).

Analysis of the cyclic anodic polarization data, presented in figure A3.1, reveals that the pitting potential of Vit 105 is the greatest, followed by $Zr_{35}Ti_{30}Be_{29}Co_6$ and $Zr_{35}Ti_{30}Be_{35}$. This suggests that the $Zr_{35}Ti_{30}Be_{35}$ is the most susceptible and $Zr_{52.5}Cu_{17.9}Ni_{14.6}Al_{10}Ti_5$ the least susceptible to attack by pitting in 0.6M NaCl. However, the corrosion current densities of the alloys with low LTM fraction are approximately two orders of magnitude lower than $Zr_{52.5}Cu_{17.9}Ni_{14.6}Al_{10}Ti_5$ in the range between E_{corr} and E_{pit}. A higher corrosion current density naturally leads to a higher corrosion rate. The corrosion rate of Vit 105 in 0.6M NaCl is reported to be 29 ± 6μm/yr [7]. By contrast, the corrosion rates of $Zr_{35}Ti_{30}Be_{29}Co_6$ and $Zr_{35}Ti_{30}Be_{35}$ in the same solution and under the same conditions were measured in this study to be 0.5 ± 0.2μm/yr and 0.9 ± 0.3μm/yr, respectively. These rates are lower than that of $Zr_{52.5}Cu_{17.9}Ni_{14.6}Al_{10}Ti_5$ by factors of ~150 °C and ~30 °C, respectively. Corrosion rates for 18/8 stainless steel, Alclad 24S-T, and annealed Monel in sea water are reported to be 13, 11.2 and 15.9μm/yr, respectively [10]. These rates are slightly lower than that of Vit 105, but more than an order of magnitude higher than the rates of $Zr_{35}Ti_{30}Be_{35}$ and $Zr_{35}Ti_{30}Be_{29}Co_6$.

The results of fatigue testing differ markedly from the corrosion results. The tested metallic glasses have similar yield strengths (1700 - 1800 MPa) and, as shown in Figure A3.2, the fatigue values at 10^7 cycles are also very close in each environment given the experimental scatter. In Table A3.1, fatigue values are presented as a fraction of the material yield strength. It is interesting to observe how each material's fatigue strength, at 10^7 cycles, diminishes in saline solution compared to air. The tested metallic glasses retain 25 - 28% of their yield strength at 10^7 cycles in air, but drop to 6 - 8% of their yield

strength in saline solution. Alclad also has a low strength in NaCl decreasing from 20% to 10%. Similar to metallic glasses, steel exhibits 25% of its strength at 10^7 cycles in air, but only drops to 15% in saline solution. Annealed Monel starts with a low yield strength, but retains the largest fractions of its yield strength surviving 10^7 cycles at 40% of its yield strength in air and 35% in saline solution.

Crack growth rates of traditional Vitreloy alloys undergoing cyclic loading in saline solutions are found to approach 1μm/cycle at high stress intensities [8], a value substantially higher than in air. Owing to the dramatically improved corrosion resistance demonstrated by $Zr_{35}Ti_{30}Be_{29}Co_6$ and $Zr_{35}Ti_{30}Be_{35}$ over the traditional Vit 105, one would expect to observe an analogous improvement in corrosion fatigue endurance as well. As seen in Table A3.1 however, no statistically significant improvement in corrosion fatigue endurance is attained. This suggests that the corrosion resistance and corrosion fatigue endurance of Vitreloy alloys are governed by distinctly different mechanisms.

When exposed in a chemical environment, Zr, the base metal for Vitreloy glasses, is known to rapidly form a passive layer several atomic distances thick that protects the bulk of the material against chemical dissolution [16-17]. Likewise, glassy Vitreloy alloys based on Zr also tend to passivate rapidly when exposed in chemical environments. The thermodynamic and chemical stability of the formed passive layer controls the rate of corrosion of these glasses and is known to be a measure of their overall corrosion resistance [18-21]. Preliminary X-ray Photoelectron Spectroscopy (XPS) studies of ZrTiBe alloys show a passive layer comprised of oxides of the base elements in ratios similar to the bulk sample [22]. This layer is stable in NaCl solutions in stress free

environments and protects the bulk sample from dissolution [20]. It is therefore reasonable to assume that the improvement in corrosion resistance demonstrated by the low LTM Vitreloy glasses ($Zr_{35}Ti_{30}Be_{29}Co_6$ and $Zr_{35}Ti_{30}Be_{35}$) over traditional Vitreloy glasses ($Zr_{52.5}Cu_{17.9}Ni_{14.6}Al_{10}Ti_5$) is due to the low fraction or complete absence of late transition metals such as Ni and Cu. The presence of late transition metals in Vitreloy glasses is known to interfere with the formation of chemically stable passive layers. For example, XPS studies of Vitreloy glasses containing Cu show that the surface composition includes Cu compounds which are not as resistant to chemical attack [22]. Under stress (or cyclic stress) corrosion conditions however, the mechanical stability of the passive layer is also important. Mechanical properties of the passive layer such as its fracture strength and fracture toughness are critical in determining the structural integrity of the layer under stress and the sustained protection of the material against chemical dissolution. While the fracture strength and fracture toughness of the passive layer of these alloys is not known, the ceramics ZrO_2 and TiO_2 have fracture strengths of 550 MPa and 52 MPa respectively, and fracture toughnesses of less than 10 MPa-$m^{1/2}$ [23]. These low fracture strength and fracture toughness values suggest that the passive layer is brittle and prone to cracking under low applied stresses.

Mechanical rupture of the passive layer can be expected to lead to severe chemical attack concentrated at the extending crack tip. Indeed, stress assisted cracking or anodic dissolution is identified to be the dominant mechanism of corrosion fatigue failure of Vitreloy glasses [7-8, 24]. Hence independent of its chemical stability, a brittle passive layer can lead to early corrosion fatigue failure despite its ability to protect against corrosion in stress free environments. Therefore, the poor corrosion fatigue performance

demonstrated by $Zr_{35}Ti_{30}Be_{29}Co_6$ and $Zr_{35}Ti_{30}Be_{35}$, despite their superior corrosion resistance in stress free environment, can be attributed to the formation of a passive layer with high chemical stability but low fracture toughness.

In conclusion, the corrosion resistance and corrosion fatigue performance of low LTM Vitreloy glasses $Zr_{35}Ti_{30}Be_{29}Co_6$ and $Zr_{35}Ti_{30}Be_{35}$ in 0.6M NaCl were investigated and compared to traditional Vitreloy glass $Zr_{52.5}Cu_{17.9}Ni_{14.6}Al_{10}Ti_5$ and to other crystalline engineering alloys used widely in saline environments such as 18/8 stainless steel, Alclad 24S-T, and annealed Monel. The low LTM Vitreloy glasses were found to exhibit corrosion rates of less than 1μm per year, which are lower by more than one order of magnitude compared to the traditional Vitreloy glass and the conventional engineering metals. The high corrosion resistance of the present alloys is attributed to the low fraction or complete absence of LTM elements facilitating the formation of a chemically stable passive layer. Despite their superb corrosion resistance, the corrosion fatigue performance of $Zr_{35}Ti_{30}Be_{29}Co_6$ and $Zr_{35}Ti_{30}Be_{35}$ is found to be rather poor, as less than 10% of their yield strength is retained at 10^7 cycles, a value comparable to traditional Vitreloy glasses but significantly lower than conventional crystalline alloys. The poor corrosion performance of the present alloys is likely due to the fracture toughness of the passive layer being relatively low, providing little protection against chemical dissolution after being fractured in a corrosive environment.

Valuable discussions with Dr. Vilupanur A. Ravi are gratefully acknowledged. This work is supported by the NSF International Materials Institutes Program under DMR-0231320, with Drs. C. Huber, U. Venkateswaran, and D. Finotello as contract monitors, and by the Office of Naval Research under ONR06-251 0566-22.

Appendix 3 References

[1] A.L. Greer, E. Ma, MRS Bull. 32 (2007) 611.
[2] W.L. Johnson, MRS Bull. 24 (1999) 42.
[3] A. Inoue, Acta Mater. 48 (2000) 279.
[4] W.L. Johnson, JOM 54 (2002) 40.
[5] Y.F. Wu, W.C. Chiang, J. Chu, T.G. Nieh, Y. Kawamura, J.K. Wu, Mater. Lett. 60 (2006) 2416.
[6] M.L. Morrison, R.A. Buchanan, R.V. Leon, C.T. Liu, B.A. Green, P.K. Liaw, J.A. Horton, J. Biomed. Mater. Res. Part A 74A (2005) 430.
[7] M.L. Morrison, R.A. Buchanan, P.K. Liaw, B.A. Green, G.Y. Wang, C.T. Liu, J.A. Horton, Mater. Sci. Eng. A 467 (2007) 198. Correspondence with the Liaw group verified that the corrosion rate value is 29 ± 6μm/yr, not 29 ± 60μm/yr as reported.
[8] V. Schroeder, C.J. Gilbert, R.O. Ritchie, Mater. Sci. Eng. A 371 (2001) 145.
[9] A. Wiest, G. Duan, M.D. Demetriou, L.A. Wiest, A. Peck, G. Kaltenboeck, B. Wiest, W.L. Johnson, Acta Mater. 56 (2008) 2625.
[10] C.V. Brouillette, Corrosion Rates in Sea Water at Port Hueneme, California, for Sixteen Metals, AD81212 Armed Services Technical Information Agency, 1954.
[11] H.E. Boyer, Atlas of Fatigue Curves, American Society for Metals, Ohio, 1986, pp. 37-38, 66, 177-180, 319, 321, 327, 391-392.
[12] H.W. Russell, L.R. Jackson, H.J. Grover, W.W. Beaver, Fatigue Strength and Related Characteristics of Aircraft Joints, National Advisory Committee for Aeronautics Technical Note No. 1485, 1948.
[13] A.C. Bond, Fatigue Studies of 24S-T and 24S-T Alclad Sheet with Various Surface Conditions, Master's Thesis, Georgia Institute of Technology, 1948.
[14] T.W. Crooker, R.E. Morey, E.A. Lange, Low Cycle Fatigue Crack Propagation Characteristics of Monel 400 and Monel K-500 Alloys, NRL Report 6218, 1965.
[15] Monel Alloy R-405, Technical Brochure, UNS N04405, www.specialmetals.com.
[16] P.A. Schweitzer, Corrosion Engineering Handbook, Marcel Dekker, Inc., New York, 1996, pp. 157-163, 195-252.
[17] D.W. White Jr., J.E. Burke, The Metal Beryllium, The American Society for Metals, Ohio, 1955, pp. 530-547.
[18] K. Hashimoto, K. Asami, M. Naka, T. Masumoto, The Research Institute for Iron, Steel and Other Metals 1694 (1979) 237.
[19] K. Hashimoto, K. Asami, M. Naka, T. Masumoto, The Research Institute for Iron, Steel and Other Metals 1695 (1979) 246.
[20] S. Hiromoto, A.P. Tsai, M. Sumita, T. Hanawa, Corros. Sci. 42 (2000) 1651.
[21] S. Hiromoto, A.P. Tsai, M. Sumita, T. Hanawa, Corros. Sci. 42 (2000) 2193.
[22] Unpublished Work.
[23] http://www.ceramics.nist.gov/srd/summary/ftmain.htm.
[24] Y. Nakai, Y. Yoshioka, JSMS 3 (2009) 219.